

Brush Polymers as Nanoscale Building Blocks for Hydrogel Synthesis

Fei Jia, Jake Song, Joshua M. Kubiak, Michika Onoda, Peter J. Santos, Koki Sano, Niels Holten-Andersen, Ke Zhang, and Robert J. Macfarlane*

Cite This: *Chem. Mater.* 2021, 33, 5748–5756

Read Online

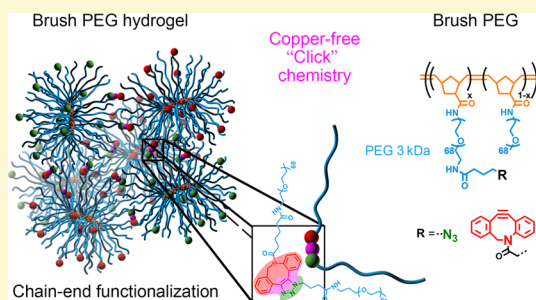
ACCESS |

Metrics & More

Article Recommendations

Supporting Information

ABSTRACT: High branch functionality (f) materials have garnered significant attention as building blocks for hydrogels as their ability to form abundant network connections yields mechanically robust gels that can potentially tolerate the negative effects of topological defects. Herein, we report the synthesis of hydrogels using brush polymers and investigate the influence of both f and polymer topology on the mechanical properties of resulting hydrogels. Our study suggests that both the high f and the extended conformation of polymer brushes that are attributed to the nanoscale shape of the brush polymers enable them to exhibit elevated gel stiffness and can effectively minimize the effects of topological defects, induce gelation at much lower cross-link concentrations, and display restrained swelling compared with gels made with more flexible polymers. In addition, because the brush polymers adopt discrete nanoparticle-like morphologies in solution, tailoring the location of the cross-linking groups at different points along the brush surface allows for different topological connectivities (e.g., side-to-side and end-to-end) to be generated, further controlling the resulting mechanical properties of the cross-linked networks. Brush polymers are therefore promising building blocks for hydrogels with highly tunable mechanical and physical properties and for the investigation of structure–property relationships affected by the gel network topology.



INTRODUCTION

Polymer hydrogels are a class of soft, highly hydrated three-dimensional networks composed of cross-linked hydrophilic polymers.^{1,2} The development of different topological structures and various cross-linking methods offers great opportunities for fabricating gels for a broad range of applications.^{3–5} Despite these successes, the influence of branch functionality (f , the average number of connections between each junction) is still being explored, partially due to the difficulties in synthesizing polymer building blocks with accurate and large values of f .

Creating a polymer network with high f is of particular interest since a greater number of connections between individual polymers can result in more mechanically robust hydrogels that are less inhibited by topological defects like dangling chains or loops.^{6–8} Prior efforts to synthesize gels that have large f have used multivalent components like hairy polymer nanoparticles or well-defined polymer structures like metal–organic cages and dendrimers. Hairy polymer nanoparticles like amphiphilic micelles and polymer-grafted nanoparticles can easily make gel structures with high f (>100).^{9,10} However, the f value cannot be tuned to a large degree of accuracy due to the nonspecific nature of connections formed between the constituent particles. Metal–organic cages (MOCs) and dendrimers are chemically and structurally well-defined and can yield polymer networks with precise f ,^{11–14} but loop defects introduced by the asymmetrical combination of MOCs/dendrimers and bivalent polymers are

inevitable, which negatively impacts the mechanical properties of resulting hydrogels. Significant information could therefore be gained from a nanoscale polymer-based building block that could express a large, controlled number of binding groups to systematically study the effects of f on gel synthesis and mechanical properties.

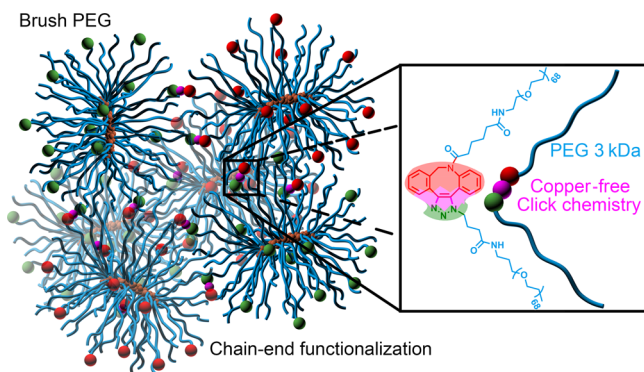
Progress over the past few decades in the development of robust polymer synthesis methods has provided a convenient building block, the brush polymer, to build hydrogels that could potentially offer insight into these research questions pertaining to connectivity within the network. Brush polymers consist of a primary polymer backbone with multiple pendent secondary side chains, where individual side chains on the brush polymers are spatially constrained and have fewer degrees of conformational freedom than linear polymers because of steric hindrance imposed by the dense packing.^{15–17} Brush polymer networks are therefore much less likely to possess cyclic defects or self-biting reactions, and complex interchain entanglements are typically diminished.^{18–20} Additionally, the number of side chains can be accurately controlled during polymerization by tuning the

Received: May 8, 2021
Revised: June 29, 2021
Published: July 7, 2021



degree of polymerization (DP). In other words, the degree of valency or f for each brush polymer can be specified as a function of the brush polymer synthesis, thereby providing a good model to study the influence of f on the hydrogel behavior. A preliminary study has now demonstrated that cross-linking the arms of water-soluble brush polymers can indeed induce interesting properties in the resulting gels.^{21,22} For example, these hydrogels exhibited rapid gelation (100-fold increase in gelation rate compared with 4-arm star polymers of an identical arm length) and nearly entirely nonswelling behavior at body temperature (~ 37 °C). Because these properties make brush polymer gels potentially beneficial in different biomedical applications, it is important to further investigate the relationship between the brush polymer design and the properties of resulting hydrogels to understand how the brush topology affects the gel behavior in a more systematic manner. Here, we report the ring-opening metathesis polymerization (ROMP) of brush polymers consisting of poly(ethylene glycol) (PEG) brushes and their subsequent gelation using “click” chemistry between azide and dibenzocyclooctyne (DBCO) groups (Scheme 1) as a means to

Scheme 1. Structure of a Brush Polymer Hydrogel^a



^aBrush polymers are crosslinked via copper-free click chemistry between azide chain ends (green spheres) and DBCO chain ends (red spheres).

elucidate such structure–property relationships and better enable topology as a design handle for controlling the gel characteristics. These brush polymer hydrogel building blocks allow for investigation into the synthesis and structure–property relationships of gels with high f polymer components as well as understanding of how the nanoscale topology of these brush polymers affects the resulting behavior of gels once formed.

RESULTS AND DISCUSSION

To study the influence of f and polymer topology on the resulting hydrogel properties, a library of random brush polymer copolymers was prepared via ROMP of two different macromonomers (3 kDa norbornene PEG terminated with either a methyl group or a Boc-protected amine, $\bar{D} < 1.05$), consisting of six different polynorbornene backbone DPs (DP = 25, 50, 75, 100, 150, and 200), and different proportions of Boc-protected side chains (between 5% and full modification of the chain ends). When these modified chains were converted to either azide- or DBCO-terminated chains, the resulting brush polymers possessed values of $f \sim 3$ –100. It is to be noted that only azide-terminated brush polymers were

synthesized with fully modified chain ends; DBCO modification above $\sim 15\%$ resulted in undesirable brush polymer aggregation due to the hydrophobic nature of the DBCO moiety. Macromonomer conversion was nearly quantitative (over 98%), and typical \bar{D} values for these polymers ranged between 1.2 and 1.7 as measured using either a DMF GPC coupled with an refractive index (RI) detector or a DMF GPC coupled with multiangle light scattering (DMF GPC-MALS) (Figure 1b and Table S1). Any unreacted macromonomers were removed during postsynthetic modification to avoid interference with the property analyses of the resulting gels (Figure S3, aqueous GPC-MALS curves of the final high-DP brush polymer product). One set of complementary 4-arm PEG polymers (synthesized via ROMP, DP and $f = 4$, 3 kDa per arm) was also synthesized as a control to allow for comparison of more common gel architectures synthesized from star polymers with lower f , allowing a better evaluation of the effects of the brush polymer topology on material properties.

Individual brush polymers were found to form discrete nanostructures under aqueous conditions with R_h (cumulant fit results) ranging from ~ 11 to ~ 35 nm as characterized by DLS (Figure 1c). This size range is consistent with the diameter observed in TEM images (Figure 1d). Additionally, brush polymers possessed similar R_h before and after chain-end modification, suggesting that limiting the extent of hydrophobic DBCO modifications to $\leq 15\%$ of the total number of chains prevented undesirable aggregation (Figure S4). The radii of gyration (R_g) were measured by aqueous GPC-MALS, and the R_g/R_h ratios for different polymers (Table S2) indicate that the polymer brushes adopted pseudospherical architectures under aqueous conditions.^{23–25} The observed pseudospherical (globular) structures are hypothesized to arise from the collapse of the hydrophobic polynorbornene backbone in the aqueous phase. Similar brush polymer systems with insoluble backbones have been reported to adopt more compact conformations (as measured both experimentally and with molecular simulations) similar to the pseudospherical, globular architectures observed here.^{23,26,27} Though high-DP brush polymers are forced to adopt a globular morphology due to the hydrophobic polynorbornene backbone, the PEG side chains on the brush polymer showed highly extended conformations as predicted based on the power law relationship between R_g and backbone DP, $R_g \sim DP^{0.7}$ (Figure S5).^{28,29}

Brush polymers were predicted to increase the stiffness of hydrogels via two different aspects of their unique structures: (1) high f ($G' \propto (f-2)/f$) as predicted by the phantom network theory for a tree-like network³⁰ and (2) rigid structure of brush polymers induced by the crowded side chains along the backbone. To first elucidate the influence of high f on gels containing brush polymers, we synthesized gels using exclusively 4-arm azide PEG and 4-arm DBCO PEG and then synthesized a series of gels (5 wt %) that substituted increasing amounts of 4-arm azide PEG with fully modified DP₂₅-azide (i.e., brush polymer with a backbone DP of 25 and 100% azide-terminated chains) (Figure 2a). It is to be noted that although 4-arm PEG and DP₂₅ polymer are not exactly equivalent in size, the difference in R_g between them is small (3.4 nm vs 6.2 nm, based on the approximation of R_h) when compared with the large R_g of other high-DP brush polymers (up to 15.9 and 25.0 nm for DP₁₀₀ and DP₂₀₀, respectively, Table S3). The effects of increasing both f and the rigidity of

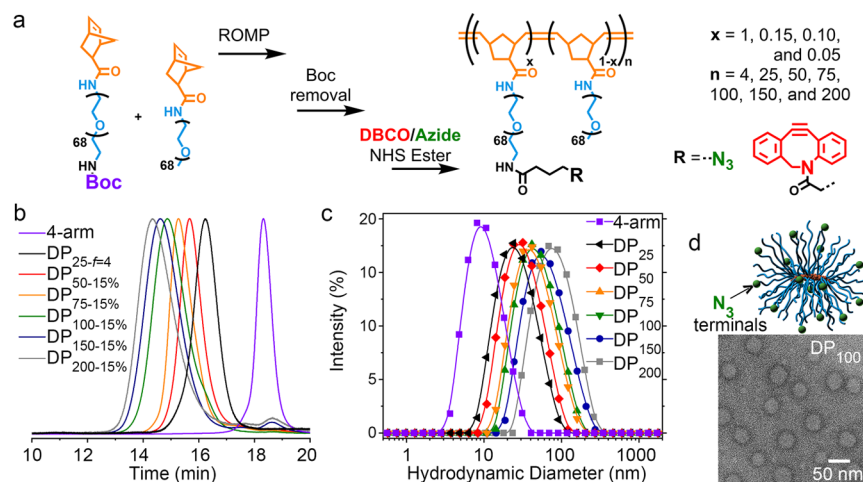


Figure 1. (a) Synthesis and postsynthetic modification of brush polymers with DBCO/azide groups. (b) *N,N*-dimethylformamide gel permeation chromatography (DMF GPC) chromatograms of brush polymers consisting of random copolymers of 15% Boc-PEG macromonomers and 85% methyl ether-terminated PEG macromonomers. GPC traces were collected using an RI detector. (c) Size distributions of selected polymers (15% DBCO end-functionalized side chains and 85% methyl ether-terminated side chains) with different DPs. Dynamic light scattering (DLS) experiments were carried out at a scattering angle of 90° at room temperature. (d) Schematic illustrations of brush polymer NPs with azide terminals. Transmission electron microscopy (TEM) images of individual brush polymers in a dilute solution (1 wt %, 15% chain-end modification, negatively stained with 1% uranyl acetate water solution).

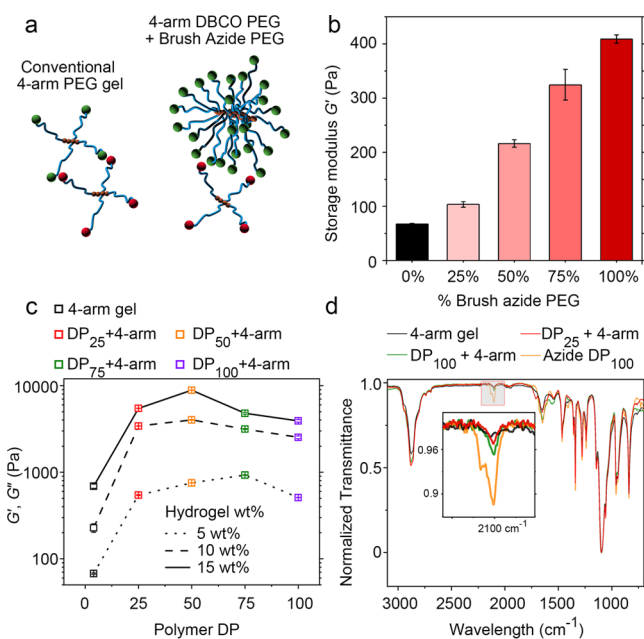


Figure 2. (a) Substituting azide-modified 4-arm PEG with an azide-terminated brush polymer in a conventional star polymer hydrogel. (b) Storage modulus change as a function of DP_{25-azide} content in the star polymer hydrogel (5 wt %). (c) Storage moduli of hydrogels cross-linked by azide-terminated brush polymers with different DPs and 4-arm PEG_{DBCO} at various polymer concentrations. (d) Fourier transform infrared (FTIR) characterization of lyophilized hydrogels with different combinations (10 wt % gels).

the polymer components simultaneously were explored by synthesizing 5, 10, and 15 wt % gels by mixing 4-arm DBCO with larger brush polymers (DP = 25, 50, 75, and 100), each with 100% azide-modified chain ends.

Hydrogels were prepared by thoroughly mixing aqueous solutions of the polymers and incubating the mixtures at room temperature overnight. Each sample was then analyzed using a rheometer to measure storage and loss moduli (G' and G'' , $\omega =$

100 to 0.1 rad/s, $\epsilon = 5\%$, and 25 °C); values of G' at 10 rad/s were used to evaluate the stiffness of the resulting hydrogels. The concentrations of both azide and DBCO reactive groups, C_r , and polymer content, wt %, were kept constant throughout all these syntheses; this was possible because the 4-arm polymers and brush polymers were synthesized using the same macromonomers, and all chains were fully modified with azide groups (Figures S2, S5, S7). Changes in G' values for the initial set of hydrogels that contained varying amounts of the 4-arm azide with azide-modified DP₂₅ (Figure 2b) indicate that the stiffness of the gels was proportional to the amount of DP_{25-azide}, ranging from ~67 Pa for the 100% 4-arm azide gels up to ~927 Pa for gels made with 100% DP_{25-azide}. The low modulus for the 4-arm gels is consistent with other similar hydrogel designs that typically use much larger amounts of 4-arm polymers to ensure the formation of a robust gel structure.³¹ While the gels formed from a mixed star polymer and brush polymers are not the lowest wt % gels that have been reported, the brush architecture clearly does exhibit some advantages in enabling the formation of stiff gels at low wt % when compared with star polymers that use the same arm length.

For the set of gels prepared with 4-arm PEG_{DBCO} and azide-modified brush polymers with increasing backbone DP, the rheological data indicate that the stiffness of hydrogels also increases with increasing backbone DP of the brush polymers (400~900 Pa vs 67 Pa at 5 wt %, 2500~4000 Pa vs 227 Pa at 10 wt %, and 4000~9000 Pa vs 690 Pa at 15 wt %, frequency sweep results; see Figure S10). These observed dramatic increases in gel stiffness for increasing DP of the brush polymer component cannot be attributed to the high f of the brush polymers alone as assumed by the phantom network model. It is important to note that side chains on brush polymers are more sterically crowded along the backbone compared with star polymers, forcing them to adopt more extended conformations as well as a rigid brush structure and thus contribute to the stiffness of the gels.³² However, the increases in G' value were not monotonic with increasing polymer DP.

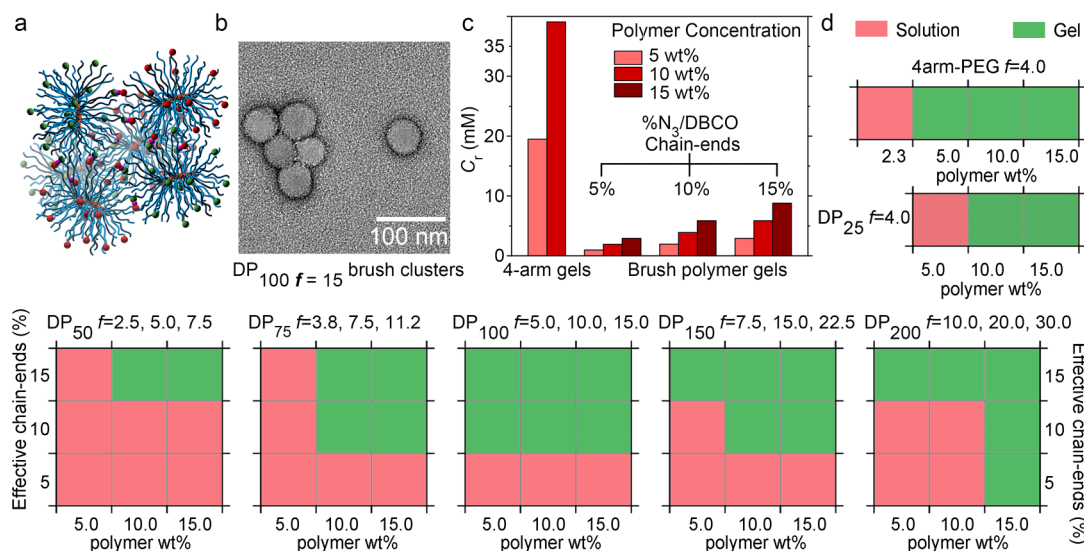


Figure 3. (a) Gels cross-linked by partially modified brush polymers. (b) TEM image of cross-linked brush polymer clusters (1 wt %) stained with 1% uranyl acetate. (c) C_r for 4-arm PEG gels and gels cross-linked by partially modified brush polymers. (d) Diagrams of a pseudo solution–gel transition observed in brush polymer network systems as a function of polymer wt % (horizontal). This transition was also examined as a function of backbone DP and the relative fraction of polymer side chains that possess azide/DBCO groups (vertical).

The increase of G' value from DP_{25} to DP_{75} was not as significant as the change from 4-arm PEG to DP_{25} , and the G' value of the gel made with DP_{100} actually decreased compared with those of any of the other brush polymer gels at all polymer concentrations tested. These data indicate that the benefits of high f have a functional limit in these brush polymer gels, and that an additional factor beyond increasing chain stiffness and average f imparts a detrimental effect on gel stiffness. We hypothesize that this factor may arise from structural defects resulting from the severe steric hindrance of high-DP brush polymers, which limits the functional chain ends of polymers from forming connections between the brush polymer and 4-arm PEG. To test this hypothesis, click reaction cross-linking yields were determined by measuring the azide peak ($\sim 2100\text{ cm}^{-1}$) by FTIR spectroscopy (Figure 2d). The FTIR data indeed indicate the presence of more non-cross-linked azide residues in the brush polymer hydrogels, especially in the case of larger brush polymer ($DP_{100\text{-azide}} + 4\text{-arm}$). Nevertheless, the G' values of brush PEG and 4-arm PEG composite gels were still much higher than that of the 4-arm PEG, further indicating that the unique morphology of brush polymers can increase the stiffness of the resulting hydrogels. Thus, using brush polymers as cross-linkers to connect more flexible star polymers results in much stiffer gels compared with traditional star polymer gels alone, with the caveat that structural defects caused by severe steric congestion of large brush polymers and the fast gelation kinetics may induce steric occlusion preventing access to all functional groups (Figure S11) and also tend to increase the number of defects, putting a limit on how much these brush polymers can improve gel stiffness. Given the uncertain influence of the collapsed hydrophobic brush polymer backbone, and possible non-Gaussian chain conformations, evaluating G' values using established hydrogel models is difficult. An optimized brush polymer design will be investigated in future studies.

To study the structural defect withstanding capability of brush polymer hydrogels, we cross-linked brush polymers with different proportions of side chains without azide/DBCO chain ends (85, 90, and 95%), that is, designed defects, and

then used a rheometer to verify gel formation; successful gels were noted as samples in which $\tan \delta = G''/G' < 1$ (at $\omega = 10\text{ rad/s}$, $\epsilon = 5\%$, and $25\text{ }^\circ\text{C}$). An additional effect of reducing the amount of modified chain ends is that the reduced concentration of reactive groups, C_r , inherently slows the gelation kinetics and allows for a more homogeneous network to be achieved, thereby mitigating the number of unreacted end groups remaining after cross-linking. Indeed, high cross-linking yields were confirmed by the complete disappearance of the azide peak by FTIR in tested gels (Figure S12). Interestingly, when DBCO- and azide-terminated brush polymers were mixed at low concentrations (1 wt %), brush polymers were still able to covalently cross-link with one another to form small clusters, as evidenced by both an increased D_h in DLS and the appearance of clusters in TEM images (Figure 3b and Figures S13 and S14). The distinct fringe between individual brush polymers in aggregated polymer clusters cast from dilute solvent mixtures (cross-linked brushes) is indicative of little to no interpenetration between brush polymer nanoparticles. In a similar study consistent with this observation, it has previously been demonstrated that large PEG clusters can be used to prepare gels with an extremely low polymer content.³³

A transition from these discrete clusters to transparent solid gels was achieved at higher concentrations (Figure S15). The pseudo solution–gel phase transition data (Figure 3d) indicate several interesting trends. Unsurprisingly, successful gelation is positively correlated with a higher effective concentration of reactive side chains, C_r , in the initial solution (0.9–8.8 mM for brush polymers and 20–40 mM for 4-arm PEG, estimated through the percentage of reactive side chains, Figure 3c) since samples with higher C_r would be expected to yield a greater density of covalent linkages. However, brush polymers were able to form gels at considerably lower values of C_r than the 4-arm controls, while the 4-arm PEG control failed to gel at $C_r = 8.8\text{ mM}$ (2.3 wt %). This difference is attributed to the much higher f of brush polymers compared to the 4-arm PEG controls. According to the Flory–Stockmayer Theory,³⁴ $\rho_c = 2/f_{\text{av}}$, where ρ_c is the critical extent of the reaction beyond

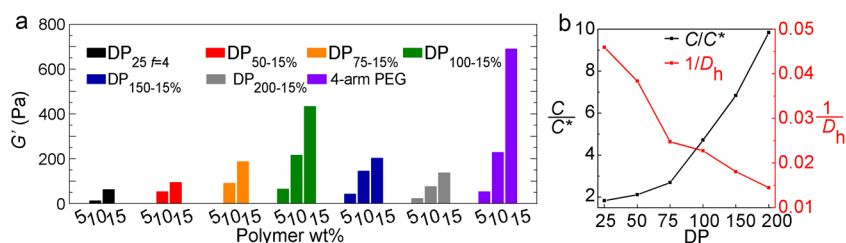


Figure 4. (a) Storage modulus G' of the brush polymer and 4-arm PEG gels as a function of polymer wt %. Of note, the low elastic moduli of hydrogels can be attributed to the low concentrations of cross-linking groups. Data from gels composed of fully chain end-modified polymers are provided in Figure 2 and Figure S10. (b) Change of C/C^* and $1/D_h$ as a function of DP at $C = 15$ wt %. Lines are a guide for the eye.

which gelation is predicted and f_{av} is the average f . Thus, gelation of high f brush polymers should require considerably lower ρ_c , which allow gelation at a lower extent of reaction.

We hypothesize another effect that enables the ability of brush polymers to form gels at low values of C_r . It stems from the fact that the brush architecture forces the PEG side chains to adopt more extended conformations, giving the brush polymers larger overall hydrodynamic radii (R_h) such that brush polymers possess significantly lower overlap concentrations (C^*) than would be expected for linear or star polymers. These low values of C^* imply that the cross-linking groups at the ends of the polymer brushes can efficiently find a bonding partner and form a connection, resulting in percolation at much lower C_r and wt %.³⁵ C^* is estimated using the equation, $C^* \approx 3M_w/4\pi N_A R_g^3$, where M_w is the weight average molecular weight of the polymer, N_A is Avogadro's number, and R_g is the radius of gyration of the brush polymer. As can be seen in this equation, R_g has the most significant influence on C^* . Therefore, increasing the R_g of the polymers using the brush architecture reduces C^* as observed in the experiments (estimated values of C^* for each polymer are listed in Table S3). As a result of these two factors, brush polymers can undergo gelation at much lower C_r than 4-arm PEGs.

Based on the high f and low estimated C^* of brush polymers obtained above, it would be tempting to conclude that increasing DP or R_h would yield more rigid gels. However, it was found that brush polymers of intermediate DP or R_h (DP₁₀₀) most readily formed viscoelastic gels across a broad range of both polymer wt % and reactive side group fractions (Figure 3d). This phenomenon was also reflected in the relationship between DP and network stiffness as the brush polymer gel G' first increased and then subsequently decreased with increasing backbone DP (Figure 4a; for detailed frequency sweep results, see Figure S17). Furthermore, when comparing brush polymer gels with the same f (i.e., the same number of cross-linking groups per polymer), DP_{100-10%} at 5 wt % gelled while DP_{200-5%} could only form gels at 15 wt %. We attribute these surprising nonmonotonic changes in G' with increasing DP to the opposing effects of C^* and cross-linking site density (ρ_{xlink} proportional to $1/D_h$).

As discussed above, increasing the backbone DP should decrease C^* , which should in turn promote gelation (Figure 4b, C/C^*). However, at the same wt % polymer, the higher DP of individual brush polymers also results in larger polymer particles and an increase in the distance between intermolecular cross-linking sites (the interfaces between covalently connected brush polymers, where each interface may contain several clickable cross-linking points). This increase in distance between brush polymers' cross-links would be expected to

reduce G' due to lower ρ_{xlink} (Figure 4b, $1/D_h$) based on the rubber elasticity theory.³⁶ For smaller brush polymers ($25 < DP < 100$), the influence of C^* and f dominates gelation and more rigid networks form as DP is increased. For larger brush polymers ($DP > 100$), however, ρ_{xlink} has a more dominant influence on the strength of the hydrogel, resulting in a reduction of G' .

Since the steric bulk of the brushes forces the brush polymer side chains into a more extended conformation compared to a more tightly coiled linear polymer, brush polymer gels were predicted to exhibit different swelling behaviors compared to the star polymer gels. Additionally, owing to the much higher number of cross-linkable polymer chains originating from each brush polymer, it was hypothesized that the brush polymer network could better withstand the mechanical strain of osmotic pressure-induced swelling than traditional gels made from more flexible components.^{37,38} To test these hypotheses, hydrogels consisting of cross-linked brush polymers and 4-arm PEG hydrogels were immersed in excess phosphate-buffered saline (PBS). Four polymer gels were selected as points of comparison: two all-brush polymer gels (DP_{100-15%} and DP_{75-15%}), a mixed 4-arm DBCO, a brush polymer azide gel (4-arm PEG_{DBCO} + DP_{100-azide}), and the 4-arm PEG-only gel; all gels were made at 10 wt %. These gels were selected for comparison as they possessed similar initial mechanical properties (DP_{100-15%} and 4-arm PEG at 10 wt %, Figure S18), same C_r (DP_{100-15%} and DP_{75-15%}), or identical chemical composition (4-arm PEG and 4-arm PEG_{DBCO} + DP_{100-azide}) despite their structural differences (Figure 5a).

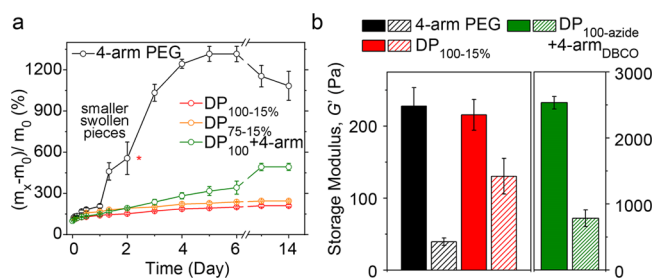


Figure 5. (a) Swelling behavior of hydrogels cross-linked by different polymer cross-linkers and (b) their mechanical properties before and after the swelling study.

Comparisons between different polymers were made on the basis of both their maximum amounts and rates of gel swelling. Note that when immersed in PBS, the 4-arm gels ruptured, forming smaller swollen parts at time points longer than 2 days of immersion. As a result, comparisons for this gel are made based on the rate of the initial swelling before gel rupture.

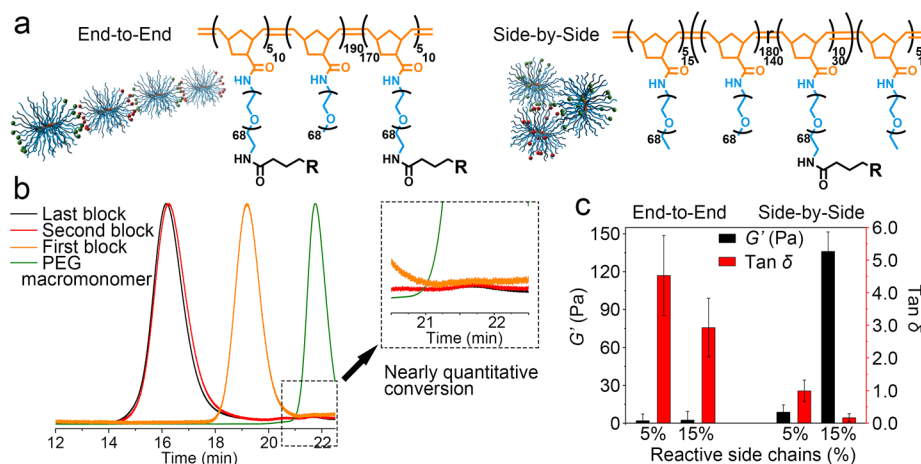


Figure 6. (a) Schematic illustration and polymer design of “end-to-end” and “side-by-side” cross-linking of polymer brushes. (b) Block-dependent DMF GPC characterization of “end-to-end” brush polymer with 15% chain-end modification (Boc group-terminated macromonomer). (c) Oscillatory rheology results for the two types of connections, 15 wt %, $\omega = 10$ rad/s, $\epsilon = 5\%$, and 25 °C.

These swelling rates were notably faster for the 4-arm PEG hydrogels than for any of the brush polymer hydrogels (Figure 5a). After 48 h, the volume of the 4-arm gel expanded by 550%, whereas the volume of the DP_{100–15%} gel only increased by 51% as determined by the wet mass change of swollen gels. After 2 weeks, the expansion of the DP_{100–15%} gel increased to a plateau of 92%, which was still less than the maximum observed expansion of the 4-arm PEG gel before its rupturing. It may initially appear that these results contradict the Flory–Rehner theory,³⁰ which predicts that the 4-arm PEG gels would exhibit less swelling than the brush polymer gel due to the assumed higher cross-linking density (higher C_r , Figure 3c) in the 4-arm PEG gel. However, bridges between cross-linking sites in the polymer brush are composed of linked PEG chains, which are in an extended state prior to gelation and swelling due to the steric constraints discussed earlier. Therefore, the addition of excess solvent should result in less expansion in response to the osmotic pressure as the linking chains are already partially extended and further extension becomes more difficult as the contour length of the chain is approached. The intermediate swelling behavior of the DP_{75–15%} gel (same C_r but looser side-chain packing compared to DP_{100–15%}) that expanded by 128% after 1 week provides further support for this hypothesis. Remarkably, the asymmetrical combination of DP₁₀₀-azide + 4-arm PEG_{DBCO} exhibited exceptional stretchability compared with a brush polymer gel in which the volume of the hydrogel expanded nearly 400% but still maintained its physical integrity. We hypothesize that this stretchability originates from the unique architecture of the high f of the brush polymer, where the multiple side chains on the brush polymer ensure the minimum amount of cross-linking needed to maintain the connectivity of the polymer network structure even though the osmotic pressure during swelling may weaken the integrity of the gel structure.

After swelling for 48 h, DP_{100–15%}, 4-arm PEG, and 4-arm PEG_{DBCO} + DP₁₀₀-azide gels were taken out and their mechanical properties were re-examined by rheological measurements. While a dramatic loss in mechanical strength was observed in the 4-arm gels after 48 h (due to reduction in volumetric cross-linking density upon swelling and the following gel breakup), the brush polymer gels possessed mechanical properties much closer to their preswollen state (Figure 5b). In particular, the G' value of 4-arm PEG dropped

from ~220 Pa to less than ~35 Pa, while the DP_{100–15%} brush polymer hydrogel maintained its elasticity as the G' value was ~130 Pa. Notably, the strength of the DP_{100–15%} gel after swelling for 48 h was ~4 times greater than that of the 4-arm PEG gel (G' of 130 Pa vs 35 Pa) (Figure 5b) though the C_r value was much lower than that of the 4-arm PEG gel. When the C_r value was at the same level, gels cross-linked by 4-arm PEG_{DBCO} and DP₁₀₀-azide possessed significantly higher G' values than 4-arm PEG gels due to high f and restrained swelling. Furthermore, the brush polymer hydrogels maintained their structure in PBS for months (Figure S19). The decreased swelling rate of the brush polymer gels along with their increased ability to maintain stiffness and coherence compared to the control gels attest to their potential for applications requiring long-term stability in hydrated environments.

In addition to the properties discussed above, the architecture of brush polymers allows for anisotropic attachment of the reactive groups to different points along the brush structure. This has previously been demonstrated to enable different connection topologies between brush polymers;^{39–41} these different connectivities would be expected to impact the gel stiffness by altering the number and location of covalent cross-links within the gel. To test this hypothesis, two versions of triblock brush polymers with an overall DP of 200 in “side-by-side” and “end-to-end” configurations (Figure 6a) were prepared. “End-to-end” polymers consist of a central block of PEG brushes without azide or DBCO functionalities (DP of 190 or 170) flanked on both ends by PEG brushes functionalized with a reactive group (DP of 5 or 15 for each block). “Side-by-side” brush polymers have the inverse design, with the middle block (DP of 190 or 170) consisting of 5 or 15% reactive side chains flanked by nonmodified PEG brushes (DP of 5 or 15). The successful installation of all three blocks was confirmed by both GPC and ¹H NMR (Figure 6b and Figure S19). Interestingly, the rheology data demonstrated that neither of the “end-to-end” brush polymers formed gels, while solid gels were obtained through the “side-by-side” cross-linking fashion (Figure 6c). This difference can be attributed to the strong steric congestion of the side chains, which causes the “end-to-end” brush polymers to behave as divalent nanostructures, preventing the branching necessary to form a three-dimensional network. Conversely, the “side-by-side”

construction is not strongly affected because the cross-links are distributed across the brush surface. While the “end-to-end” topology failed to yield a hydrogel (frequency sweep result, Figure S21), a marked increase in the viscosity of the polymer solution was observed; future studies will investigate these complex fluids to determine the extent of tunability in viscosity as a function of anisotropic brush polymer cross-linking. Recently, interest has been growing in accurately synthesizing polymers with specific architectural designs, such as asymmetrical miktoarm polymers⁴² or branched polymers.⁴³ Together with these design methods, the ability to sequentially polymerize backbone residues bearing side chains of different functionalities opens up the possibility of regioselectivity modifying individual polymer chains. The presented findings indicate a potential route to controlling the manner in which these designer macromolecules are connected into larger networks.

CONCLUSIONS

In this study, we have elucidated how the brush polymer topology can be used to tune the physical properties of hydrogel materials. Our data show that high f brush polymers can form hydrogels even at low polymer wt %, owing to the large number of functional groups present across the brush polymer. The nanoparticle-sized brush polymers therefore allow for gelation at much lower cross-linking concentrations, even with extremely high proportions of topological defects. However, when the size of the brush polymer is above a certain threshold, the long distance between the cross-linking sites in the resulting gels counteracts the effect of reduced C^* , diminishing the mechanical properties of the resulting gels. In addition, the reduced swelling rate and better retention of mechanical properties after swelling attributed to the dense packing of the side chains all indicate that brush polymer gels hold great potential for long-term use-related applications. Importantly, because the interesting properties observed in these polymer gels are derived from the brush architecture, the use of polymer brushes as gel building blocks should also be extendable to multiple polymer compositions, including thermosets, thermoplastics, and elastomers. The inherent properties of polymer brushes are therefore an interesting tool for the exploration of structure–property relationships and use in a variety of applications, such as multifunctional cross-linkers for robust adhesives and 3D cell cultures with a minimal osmotic pressure.

EXPERIMENTAL METHODS

Detailed descriptions of the methods are provided in the Supporting Information; a brief discussion is provided here for reference.

Synthesis and Gelation of Brush Polymers. Brush polymers were synthesized using the reported ROMP protocols. Generally, norbornene-terminated PEG monomers were polymerized using the modified 2nd generation Grubbs catalyst in anhydrous dichloromethane (Sections 2.1, 2.2, Supporting Information). Upon removal of Boc protecting groups, brush polymers were further modified with azide or DBCO functional groups via an esterification reaction (Section 2.3, Supporting Information). Hydrogels were obtained by mixing DBCO- and azide-modified polymers, and the related mechanical properties were measured using an Anton Paar rheometer (Sections 2.5, 2.6, Supporting Information).

Swelling Measurement. Selected polymer samples were gelled in centrifuge tubes and immersed in PBS buffer. The swollen state was calculated based on the mass gained at each time point (Section 2.7, Supporting Information).

“Side-by-Side” and “End-to-End” Connected Brush Polymer Networks. Two versions of triblock brush polymers were synthesized using the same ROMP protocols (Section 2.2, Supporting Information). The completion of each polymer block was confirmed using a DMF GPC. The same gelation process and viscoelastic characterizations were performed to study their related properties.

Instrumentation and Data Collection. Polydispersity and macromonomer conversion of the synthesized brush polymers were characterized using a DMF GPC (TOSOH EcoSEC HLC-8320, 0.05 M LiBr, calibrated with ReadyCal-Kit PEO/PEG, PSS-Polymer Standards Service - USA Inc). D_h of polymer particles was measured using a dual-angle DLS Malvern Zetasizer Nano ZSP and a single-angle DLS Wyatt Dyna Pro Plate Reader. R_g of polymer particles was measured using an aqueous GPC-MALS (Agilent Technologies 1260 Infinity system using two Aquagel columns in water with 0.02% sodium azide as the mobile phase; GPC signals were collected using Wyatt light scattering and refractive index detectors). Dry-state morphologies of brush polymers were imaged using an FEI Tecnai Multipurpose Digital TEM electron microscope utilizing an accelerating voltage of 120 kV. Installation of functional groups was confirmed by ¹H NMR (Bruker Avance III HD Nanobay spectrometer), UV–vis spectroscopy (Varian Cary 5000), and FTIR (PerkinElmer Model 2000). An Anton Paar rheometer with a parallel plate geometry (PP-10 probe, 10 mm diameter, flat) was used to characterize the dynamic properties of the polymer network samples.

ASSOCIATED CONTENT

Supporting Information

The Supporting Information is available free of charge at <https://pubs.acs.org/doi/10.1021/acs.chemmater.1c01585>.

Materials, experimental procedures, synthetic schemes, characterizations of brush polymers (FTIR, UV–vis, TEM, GPC, and DLS), rheology data for the polymer networks, and supplementary figures (PDF)

AUTHOR INFORMATION

Corresponding Author

Robert J. Macfarlane – Department of Materials Science and Engineering, Massachusetts Institute of Technology, Cambridge, Massachusetts 02139, United States; orcid.org/0000-0001-9449-2680; Email: rmacfarl@mit.edu

Authors

Fei Jia – Department of Materials Science and Engineering, Massachusetts Institute of Technology, Cambridge, Massachusetts 02139, United States

Jake Song – Department of Materials Science and Engineering, Massachusetts Institute of Technology, Cambridge, Massachusetts 02139, United States; orcid.org/0000-0003-1254-6206

Joshua M. Kubiak – Department of Materials Science and Engineering, Massachusetts Institute of Technology, Cambridge, Massachusetts 02139, United States

Michika Onoda – Department of Materials Science and Engineering, Massachusetts Institute of Technology, Cambridge, Massachusetts 02139, United States

Peter J. Santos – Department of Materials Science and Engineering, Massachusetts Institute of Technology, Cambridge, Massachusetts 02139, United States

Koki Sano – Department of Materials Science and Engineering, Massachusetts Institute of Technology, Cambridge, Massachusetts 02139, United States

Niels Holten-Andersen – Department of Materials Science and Engineering, Massachusetts Institute of Technology,

Cambridge, Massachusetts 02139, United States;

orcid.org/0000-0002-5318-9674

Ke Zhang – Department of Chemistry and Chemical Biology, Northeastern University, Boston, Massachusetts 02115, United States; orcid.org/0000-0002-8142-6702

Complete contact information is available at:

<https://pubs.acs.org/10.1021/acs.chemmater.1c01585>

Author Contributions

The manuscript was written through contributions of all authors. All authors have given approval to the final version of the manuscript.

Notes

The authors declare no competing financial interest.

ACKNOWLEDGMENTS

This study was supported by the MRSEC Program of the National Science Foundation under award DMR 1419807 and made use of the MRSEC Shared Experimental Facilities at MIT. The authors thank the Koch Institute Swanson Biotechnology Center for technical support, specifically the Peterson Nanotechnology Materials Core Facility. The authors also thank Sarah Av-Ron at MIT for help with GPC measurements. K.Z. acknowledges support by the National Institutes of Health (the National Institute of General Medical Sciences Award Number 1R01GM121612-01) and the National Science Foundation (CAREER Award Number 1453255). M.O. is supported by JSPS KAKENHI Grant Numbers 16J09350 and 20K15341.

REFERENCES

- (1) Ahmed, E. M. Hydrogel: Preparation, Characterization, and Applications: A Review. *J. Adv. Res.* **2015**, *6*, 105–121.
- (2) Laftah, W. A.; Hashim, S.; Ibrahim, A. N. Polymer Hydrogels: A Review. *Polym.-Plast. Technol. Eng.* **2011**, *50*, 1475–1486.
- (3) Nonoyama, T.; Wada, S.; Kiyama, R.; Kitamura, N.; Mredha, M. T. I.; Zhang, X.; Kurokawa, T.; Nakajima, T.; Takagi, Y.; Yasuda, K.; Gong, J. P. Double-Network Hydrogels Strongly Bondable to Bones by Spontaneous Osteogenesis Penetration. *Adv. Mater.* **2016**, *28*, 6740–6745.
- (4) Bin Imran, A.; Esaki, K.; Gotoh, H.; Seki, T.; Ito, K.; Sakai, Y.; Takeoka, Y. Extremely Stretchable Thermosensitive Hydrogels by Introducing Slide-Ring Polyrotaxane Cross-Linkers and Ionic Groups into the Polymer Network. *Nat. Commun.* **2014**, *5*, 5124.
- (5) Gong, J. P.; Katsuyama, Y.; Kurokawa, T.; Osada, Y. Double-Network Hydrogels with Extremely High Mechanical Strength. *Adv. Mater.* **2003**, *15*, 1155–1158.
- (6) Gu, Y.; Zhao, J.; Johnson, J. A. A (Macro)Molecular-Level Understanding of Polymer Network Topology. *Trends. Chem.* **2019**, *1*, 318–334.
- (7) Kawamoto, K.; Zhong, M.; Wang, R.; Olsen, B. D.; Johnson, J. A. Loops versus Branch Functionality in Model Click Hydrogels. *Macromolecules* **2015**, *48*, 8980–8988.
- (8) Zhong, M.; Wang, R.; Kawamoto, K.; Olsen, B. D.; Johnson, J. A. Quantifying the Impact of Molecular Defects on Polymer Network Elasticity. *Science* **2016**, *353*, 1264–1268.
- (9) Wang, Y.; Chen, L.; Tan, L.; Zhao, Q.; Luo, F.; Wei, Y.; Qian, Z. PEG–PCL Based Micelle Hydrogels as Oral Docetaxel Delivery Systems for Breast Cancer Therapy. *Biomaterials* **2014**, *35*, 6972–6985.
- (10) Chen, Y.; Pang, X.-H.; Dong, C.-M. Dual Stimuli-Responsive Supramolecular Polypeptide-Based Hydrogel and Reverse Micellar Hydrogel Mediated by Host–Guest Chemistry. *Adv. Funct. Mater.* **2010**, *20*, 579–586.
- (11) Zhukhovitskiy, A. V.; Zhong, M.; Keeler, E. G.; Michaelis, V. K.; Sun, J. E. P.; Hore, M. J. A.; Pochan, D. J.; Griffin, R. G.; Willard, A. P.; Johnson, J. A. Highly Branched and Loop-Rich Gels via Formation of Metal–Organic Cages Linked by Polymers. *Nat. Chem.* **2016**, *8*, 33–41.
- (12) Gu, Y.; Alt, E. A.; Wang, H.; Li, X.; Willard, A. P.; Johnson, J. A. Photoswitching Topology in Polymer Networks with Metal–Organic Cages as Crosslinks. *Nature* **2018**, *560*, 65–69.
- (13) Wang, Q.; Mynar, J. L.; Yoshida, M.; Lee, E.; Lee, M.; Okuro, K.; Kinbara, K.; Aida, T. High-Water-Content Mouldable Hydrogels by Mixing Clay and a Dendritic Molecular Binder. *Nature* **2010**, *463*, 339–343.
- (14) Marmillon, C.; Gauffre, F.; Gulik-Krzywicki, T.; Loup, C.; Caminade, A.-M.; Majoral, J.-P.; Vors, J.-P.; Rump, E. Organophosphorus Dendrimers as New Gelators for Hydrogels. *Angew. Chem., Int. Ed.* **2001**, *40*, 2626–2629.
- (15) Banquy, X.; Burdyńska, J.; Lee, D. W.; Matyjaszewski, K.; Israelachvili, J. Bioinspired Bottle-Brush Polymer Exhibits Low Friction and Amontons-like Behavior. *J. Am. Chem. Soc.* **2014**, *136*, 6199–6202.
- (16) Verduzco, R.; Li, X.; Pesek, S. L.; Stein, G. E. Structure, Function, Self-Assembly, and Applications of Bottlebrush Copolymers. *Chem. Soc. Rev.* **2015**, *44*, 2405–2420.
- (17) Müllner, M.; Müller, A. H. E. Cylindrical Polymer Brushes – Anisotropic Building Blocks, Unimolecular Templates and Particulate Nanocarriers. *Polymer* **2016**, *98*, 389–401.
- (18) Daniel, W. F. M.; Burdyńska, J.; Vatankhah-Varnoosfaderani, M.; Matyjaszewski, K.; Paturej, J.; Rubinstein, M.; Dobrynin, A. V.; Sheiko, S. S. Solvent-Free, Supersoft and Superelastic Bottlebrush Melts and Networks. *Nat. Mater.* **2016**, *15*, 183–189.
- (19) Vatankhah-Varnoosfaderani, M.; Daniel, W. F. M.; Zhushma, A. P.; Li, Q.; Morgan, B. J.; Matyjaszewski, K.; Armstrong, D. P.; Spontak, R. J.; Dobrynin, A. V.; Sheiko, S. S. Bottlebrush Elastomers: A New Platform for Freestanding Electroactuation. *Adv. Mater.* **2017**, *29*, No. 1604209.
- (20) Adamiak, L.; Touve, M. A.; LeGuyader, C. L. M.; Gianneschi, N. C. Peptide Brush Polymers and Nanoparticles with Enzyme-Regulated Structure and Charge for Inducing or Evading Macrophage Cell Uptake. *ACS Nano* **2017**, *11*, 9877–9888.
- (21) Jia, F.; Kubiak, J. M.; Onoda, M.; Wang, Y.; Macfarlane, R. J. Design and Synthesis of Quick Setting Non-Swelling Hydrogels via Brush Polymers. *Adv. Sci.* **2021**, No. 2100968.
- (22) Nakagawa, S.; Yoshie, N. Synthesis of a Bottlebrush Polymer Gel with a Uniform and Controlled Network Structure. *ACS Macro Lett.* **2021**, *10*, 186–191.
- (23) Lu, X.; Jia, F.; Tan, X.; Wang, D.; Cao, X.; Zheng, J.; Zhang, K. Effective Antisense Gene Regulation via Noncationic, Polyethylene Glycol Brushes. *J. Am. Chem. Soc.* **2016**, *138*, 9097–9100.
- (24) Jia, F.; Lu, X.; Tan, X.; Wang, D.; Cao, X.; Zhang, K. Effect of PEG Architecture on the Hybridization Thermodynamics and Protein Accessibility of PEGylated Oligonucleotides. *Angew. Chem., Int. Ed.* **2017**, *56*, 1239–1243.
- (25) Johnson, J. A.; Lu, Y. Y.; Burts, A. O.; Xia, Y.; Durrell, A. C.; Tirrell, D. A.; Grubbs, R. H. Drug-Loaded, Bivalent-Bottle-Brush Polymers by Graft-through ROMP. *Macromolecules* **2010**, *43*, 10326–10335.
- (26) Jia, F.; Lu, X.; Wang, D.; Cao, X.; Tan, X.; Lu, H.; Zhang, K. Depth-Profiling the Nuclease Stability and the Gene Silencing Efficacy of Brush-Architected Poly(Ethylene Glycol)–DNA Conjugates. *J. Am. Chem. Soc.* **2017**, *139*, 10605–10608.
- (27) Zhang, M.; Müller, A. H. E. Cylindrical Polymer Brushes. *J. Polym. Sci., Part A: Polym. Chem.* **2005**, *43*, 3461–3481.
- (28) Moh, L. C. H.; Losego, M. D.; Braun, P. V. Solvent Quality Effects on Scaling Behavior of Poly(Methyl Methacrylate) Brushes in the Moderate- and High-Density Regimes. *Langmuir* **2011**, *27*, 3698–3702.
- (29) Reith, D.; Müller, B.; Müller-Plathe, F.; Wiegand, S. How Does the Chain Extension of Poly (Acrylic Acid) Scale in Aqueous

Solution? A Combined Study with Light Scattering and Computer Simulation. *J. Chem. Phys.* **2002**, *116*, 9100–9106.

(30) Flory, P. J.; Rehner, J., Jr. Statistical Mechanics of Cross-Linked Polymer Networks II. Swelling. *J. Chem. Phys.* **1943**, *11*, 521–526.

(31) Sakai, T.; Matsunaga, T.; Yamamoto, Y.; Ito, C.; Yoshida, R.; Suzuki, S.; Sasaki, N.; Shibayama, M.; Chung, U. Design and Fabrication of a High-Strength Hydrogel with Ideally Homogeneous Network Structure from Tetrahedron-like Macromonomers. *Macromolecules* **2008**, *41*, 5379–5384.

(32) Keith, A. N.; Vatankhah-Varnosfaderani, M.; Clair, C.; Fahimipour, F.; Dashtimoghadam, E.; Lallam, A.; Sztucki, M.; Ivanov, D. A.; Liang, H.; Dobrynin, A. V.; Sheiko, S. S. Bottlebrush Bridge between Soft Gels and Firm Tissues. *ACS Cent. Sci.* **2020**, *6*, 413–419.

(33) Hayashi, K.; Okamoto, F.; Hoshi, S.; Katashima, T.; Zujur, D. C.; Li, X.; Shibayama, M.; Gilbert, E. P.; Chung, U.; Ohba, S.; Oshika, T.; Sakai, T. Fast-Forming Hydrogel with Ultralow Polymeric Content as an Artificial Vitreous Body. *Nat. Biomed. Eng.* **2017**, *1*, No. 0044.

(34) Stockmayer, W. H. Theory of Molecular Size Distribution and Gel Formation in Branched Polymers II. General Cross Linking. *J. Chem. Phys.* **1944**, *12*, 125–131.

(35) Ying, Q.; Chu, B. Overlap Concentration of Macromolecules in Solution. *Macromolecules* **1987**, *20*, 362–366.

(36) Anseth, K. S.; Bowman, C. N.; Brannon-Peppas, L. Mechanical Properties of Hydrogels and Their Experimental Determination. *Biomaterials* **1996**, *17*, 1647–1657.

(37) Kirchof, S.; Brandl, F. P.; Hammer, N.; Goepferich, A. M. Investigation of the Diels–Alder Reaction as a Cross-Linking Mechanism for Degradable Poly(Ethylene Glycol) Based Hydrogels. *J. Mater. Chem. B* **2013**, *1*, 4855–4864.

(38) García-Astrain, C.; Avérous, L. Synthesis and Behavior of Click Cross-Linked Alginate Hydrogels: Effect of Cross-Linker Length and Functionality. *Int. J. Biol. Macromol.* **2019**, *137*, 612–619.

(39) Lu, X.; Watts, E.; Jia, F.; Tan, X.; Zhang, K. Polycondensation of Polymer Brushes via DNA Hybridization. *J. Am. Chem. Soc.* **2014**, *136*, 10214–10217.

(40) Kawamoto, K.; Zhong, M.; Gadelrab, K. R.; Cheng, L.-C.; Ross, C. A.; Alexander-Katz, A.; Johnson, J. A. Graft-through Synthesis and Assembly of Janus Bottlebrush Polymers from A-Branch-B Diblock Macromonomers. *J. Am. Chem. Soc.* **2016**, *138*, 11501–11504.

(41) Foster, J. C.; Varlas, S.; Couturaud, B.; Coe, Z.; O'Reilly, R. K. Getting into Shape: Reflections on a New Generation of Cylindrical Nanostructures' Self-Assembly Using Polymer Building Blocks. *J. Am. Chem. Soc.* **2019**, *141*, 2742–2753.

(42) Levi, A. E.; Fu, L.; Lequieu, J.; Horne, J. D.; Blankenship, J.; Mukherjee, S.; Zhang, T.; Fredrickson, G. H.; Gutekunst, W. R.; Bates, C. M. Efficient Synthesis of Asymmetric Miktoarm Star Polymers. *Macromolecules* **2020**, *53*, 702–710.

(43) Lunn, D. J.; Seo, S.; Lee, S.-H.; Zerdan, R. B.; Mattson, K. M.; Treat, N. J.; McGrath, A. J.; Gutekunst, W. R.; Lawrence, J.; Abdilla, A.; Anastasaki, A.; Knight, A. S.; Schmidt, B. V. K. J.; Bates, M. W.; Clark, P. G.; DeRocher, J. P.; Dyk, A. K. V.; Hawker, C. J. Scalable Synthesis of an Architectural Library of Well-Defined Poly(Acrylic Acid) Derivatives: Role of Structure on Dispersant Performance. *J. Polym. Sci., Part A: Polym. Chem.* **2019**, *57*, 716–725.